Technical note: Adaptably diagnosing O_3-NO_x-VOC sensitivity evolution with routine pollution and meteorological data

Minjuan Huang[1,2 *], Tengchao Liao [1,2]

1. School of Atmospheric Sciences, Sun Yat-sen University, and Southern Marine Science and Engineering Guangdong Laboratory (Zhuhai), Zhuhai 519082, PR China

2. Guangdong Provincial Observation and Research Station for Climate Environment and Air Quality Change in the Pearl River Estuary, Key Laboratory of Tropical Atmosphere-Ocean System (Sun Yat-sen University), Ministry of Education, Zhuhai, 519082, PR China

* Corresponding author's e-mail: hminjuan@mail.sysu.edu.cn

S1. Comparison of fitting significance amongst parametric models

Although all the *log-Poly2* fits (Equation 7) were convergent and effective, quite certain portion of them did not achieve the statistical significance (p > 0.1) (Figures S11-S12 (g)). The other six models (Equations 1-6) generally performed well in capturing the maximum DPO_3 and partition point, with most fits achieving the statistical significance ($p \leq 0.1$) for the parameters d (representing the maximum DPO_3) as well as Xo, $log(X)_o$ and e (indicative of the partition points) (Figures S11-S12 (a-f)). The regression of the parameter b, related to the curve width, was generally more statistically significant based on the *log-Bragg3* and *log-Lorentz3* models (Figures S11-S12 (c, e)). The baseline of the DPO_3−NO_2 (or NO_x) diagram is expected to be near zero; and only the *log-Bragg4* and *log-Lorentz4* models incorporate the curve baseline related parameter c. However, both the regressing baselines varied significantly across fits and regions (Figures S2-S6 and S8-S9 (d, f)), and quite portion of them did not exhibit statistically significant (p > 0.1) (Figures S11-S12 (d, f)). Amongst all models, only the *Beta* and *log-Beta* models can fit a skew curve; and they are confined by both the minimum and maximum thresholds of NO_2 (or NO_x), represented by the parameters of X_b (or $log(X)_b$) and X_c (or $log(X)_c$), respectively. However, most of the regressions for these parameters were not statistically significant (p > 0.1) (Figures S11- S12 (a, b)). In summary, the *log-Bragg3* and *log-Lorentz3* models were the most statistically significant in characterizing the regular DPO_3-NO_x (or NO_2) relation, with over 95% of fits achieving the statistical significance (p < 0.1) (Figures S11-S12 (c, e)).

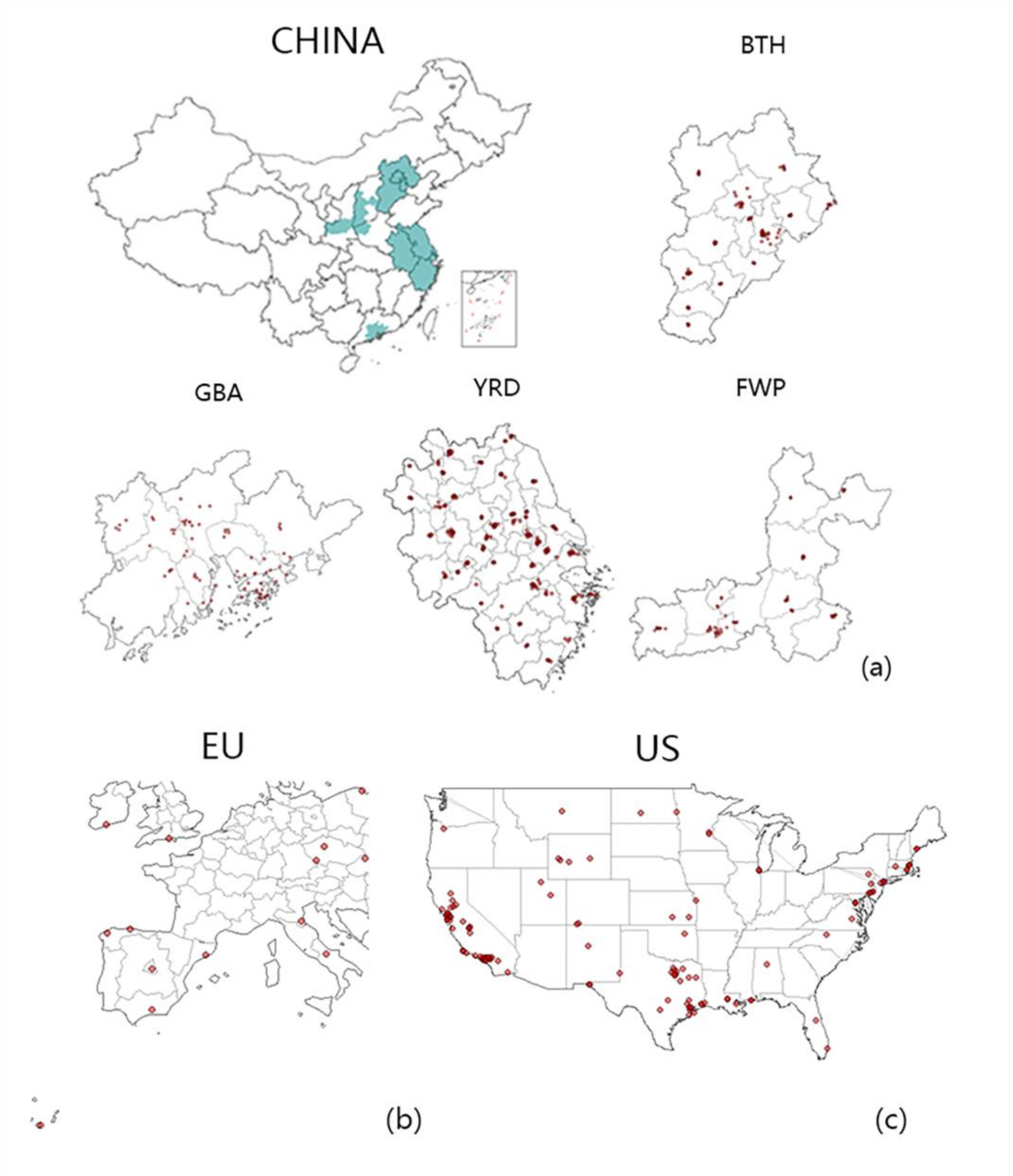

Figure S1 Locations of the studied pollution monitoring stations

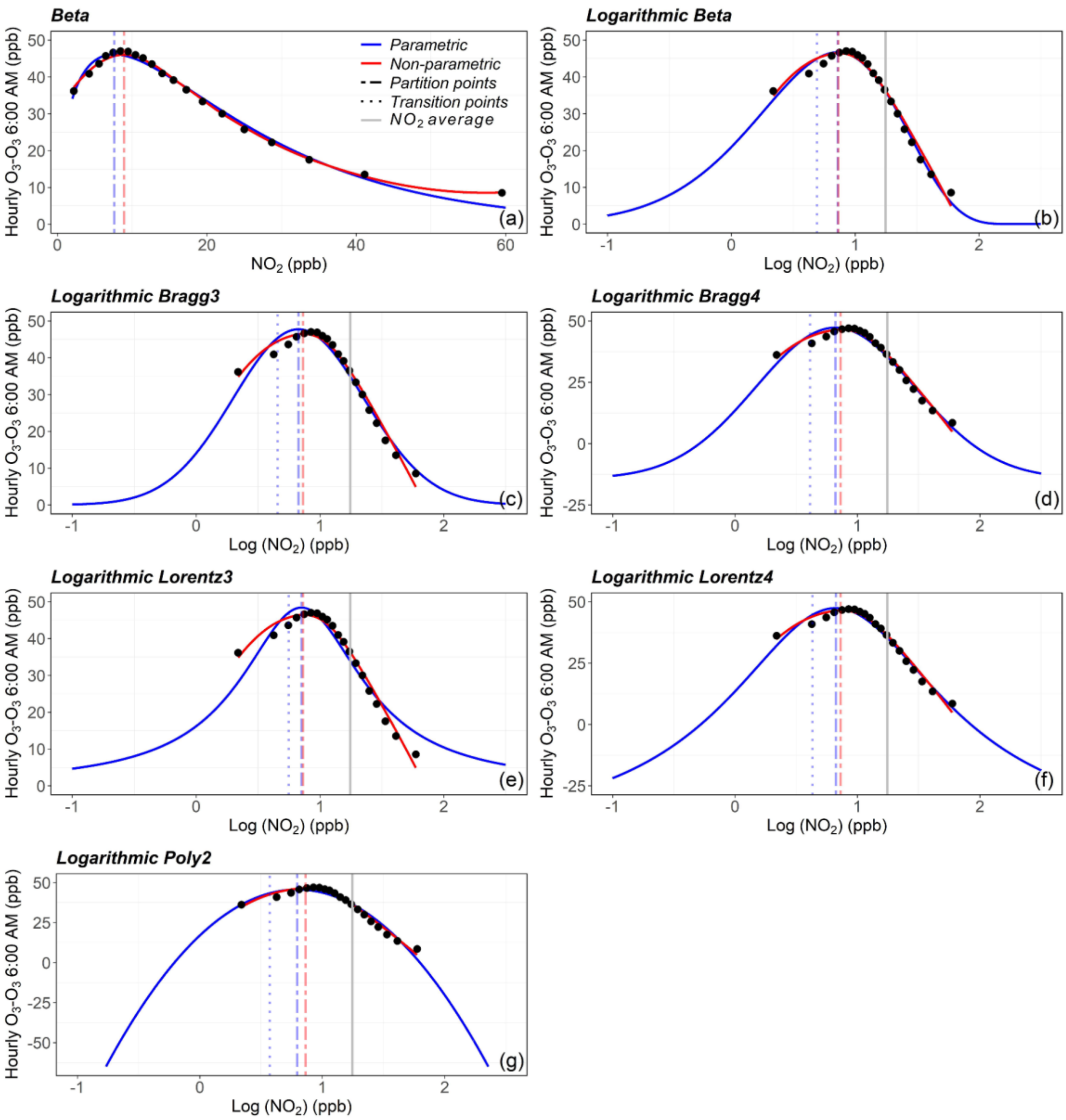

Figure S2 The **DPO_3-NO_2** curves for the **BTH** region (2014-2019) individually fitted by the studied models (Equations 1-7)

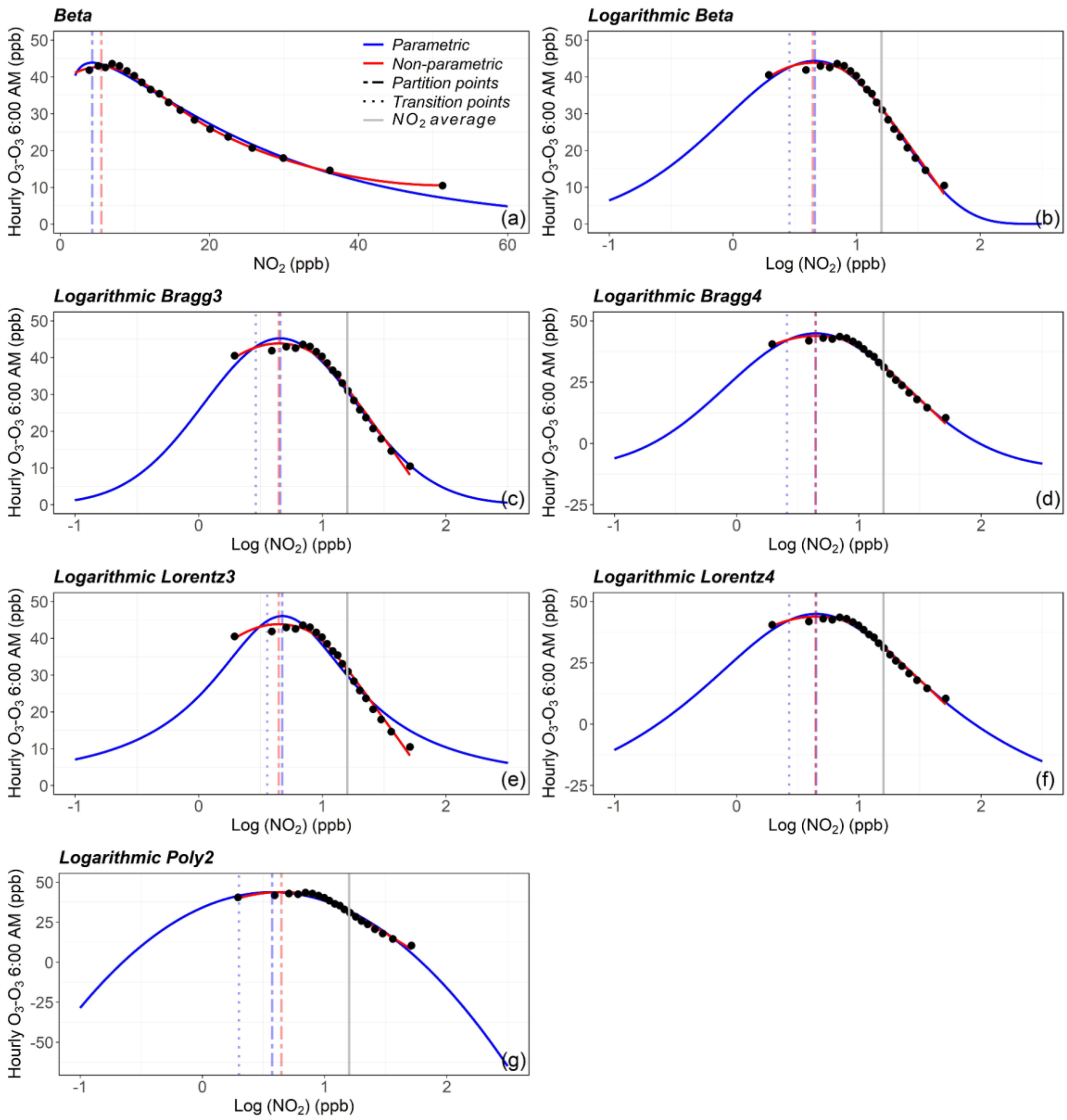

Figure S3 The **DPO_3-NO_2** curves for the **FWP** region (2014-2019) individually fitted by the studied models (Equations 1-7)

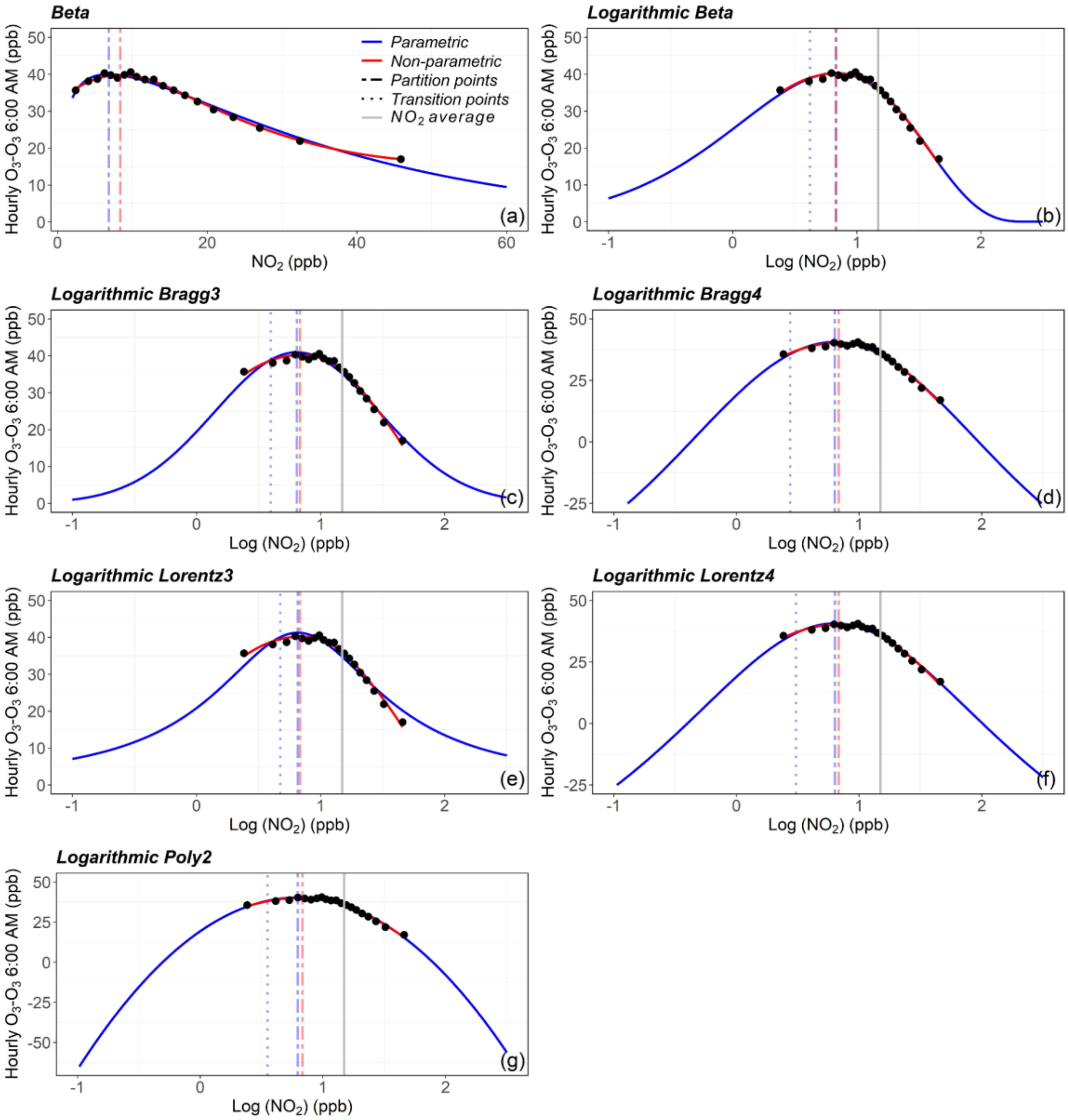

Figure S4 The **DPO3-NO2** curves for the **YRD** region (2014-2019) individually fitted by the studied models (Equations 1-7)

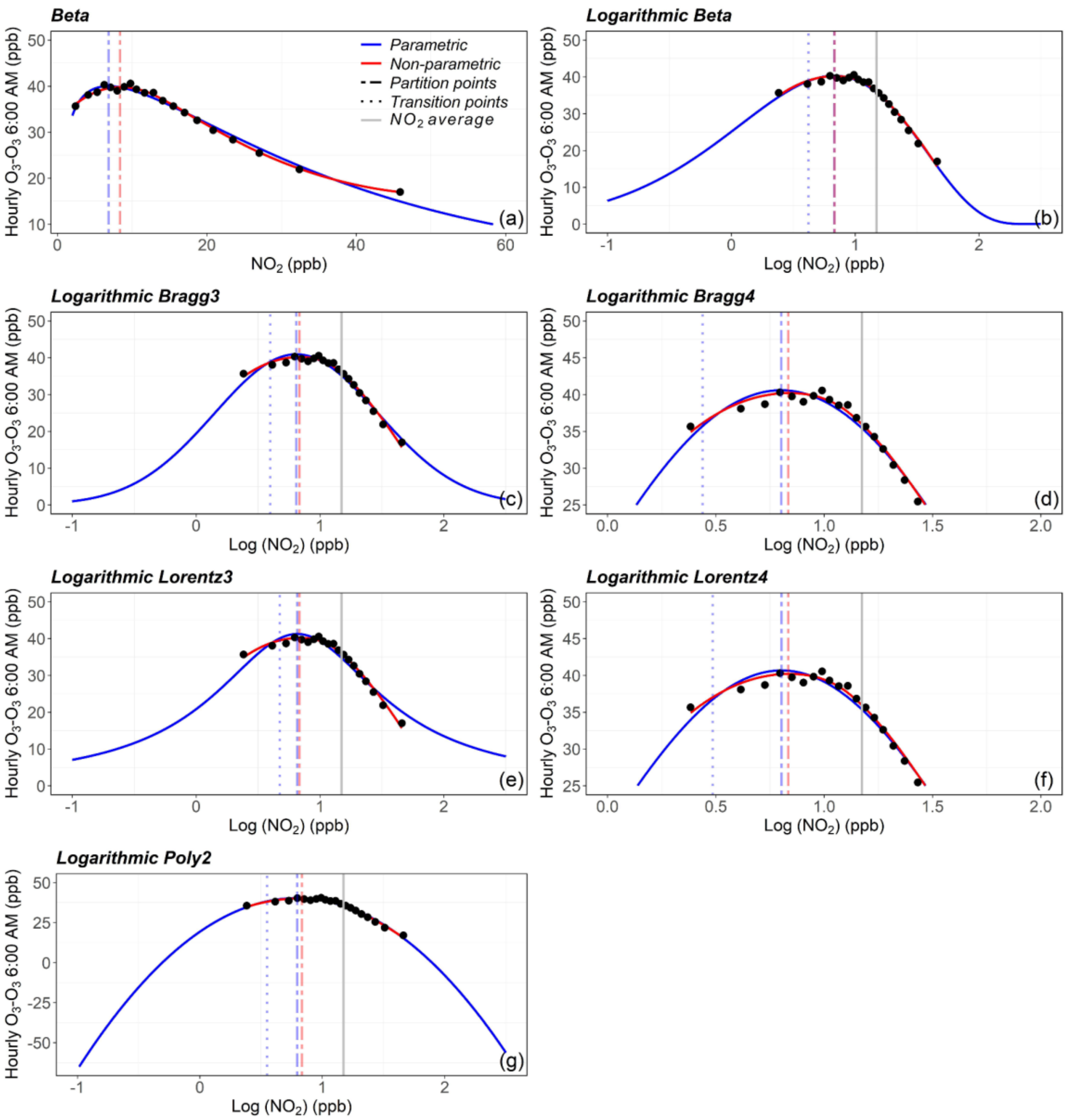

Figure S5 The **DPO_3-NO_2** curves for the **PRD** region (2014-2019) individually fitted by the studied models (Equations 1-7)

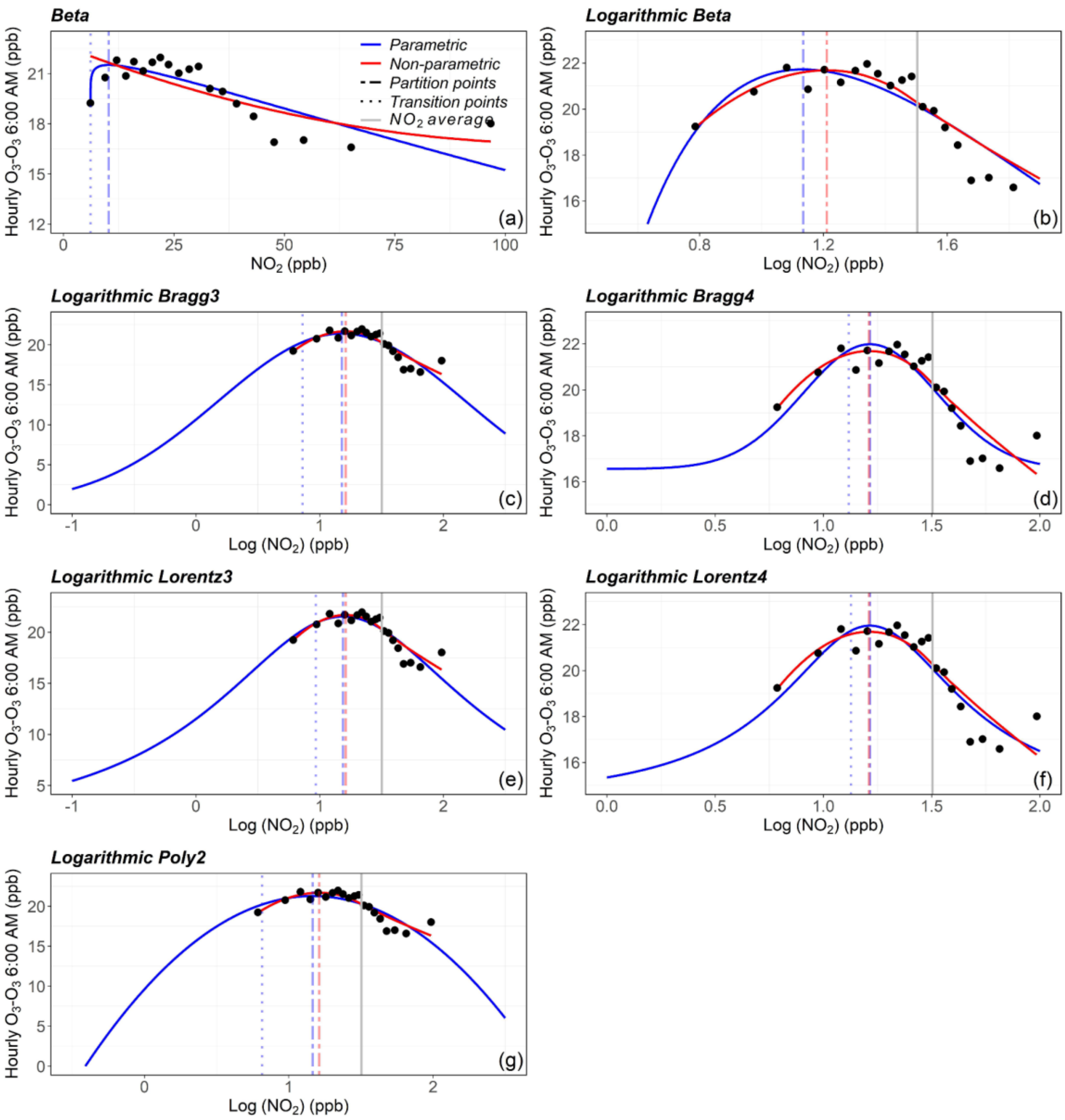

Figure S6 The **DPO_3-NO_2** curves for the **Hong Kong** (2014-2019) individually fitted by the studied models (Equations 1-7)

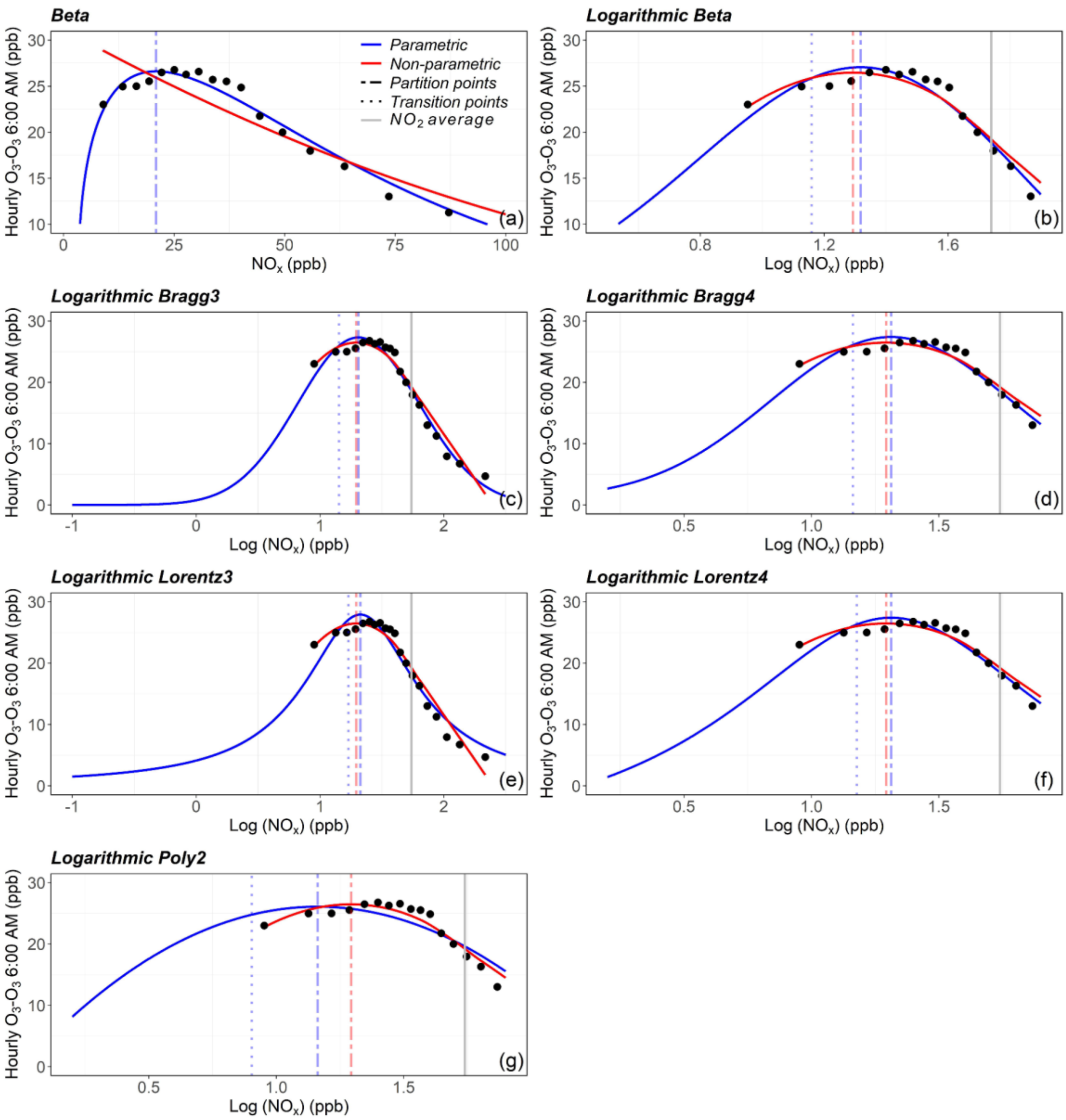

Figure S7 The **DPO_3-NO_x** curves for the **Hong Kong** (2014-2019) individually fitted by the studied models (Equations 1-7)

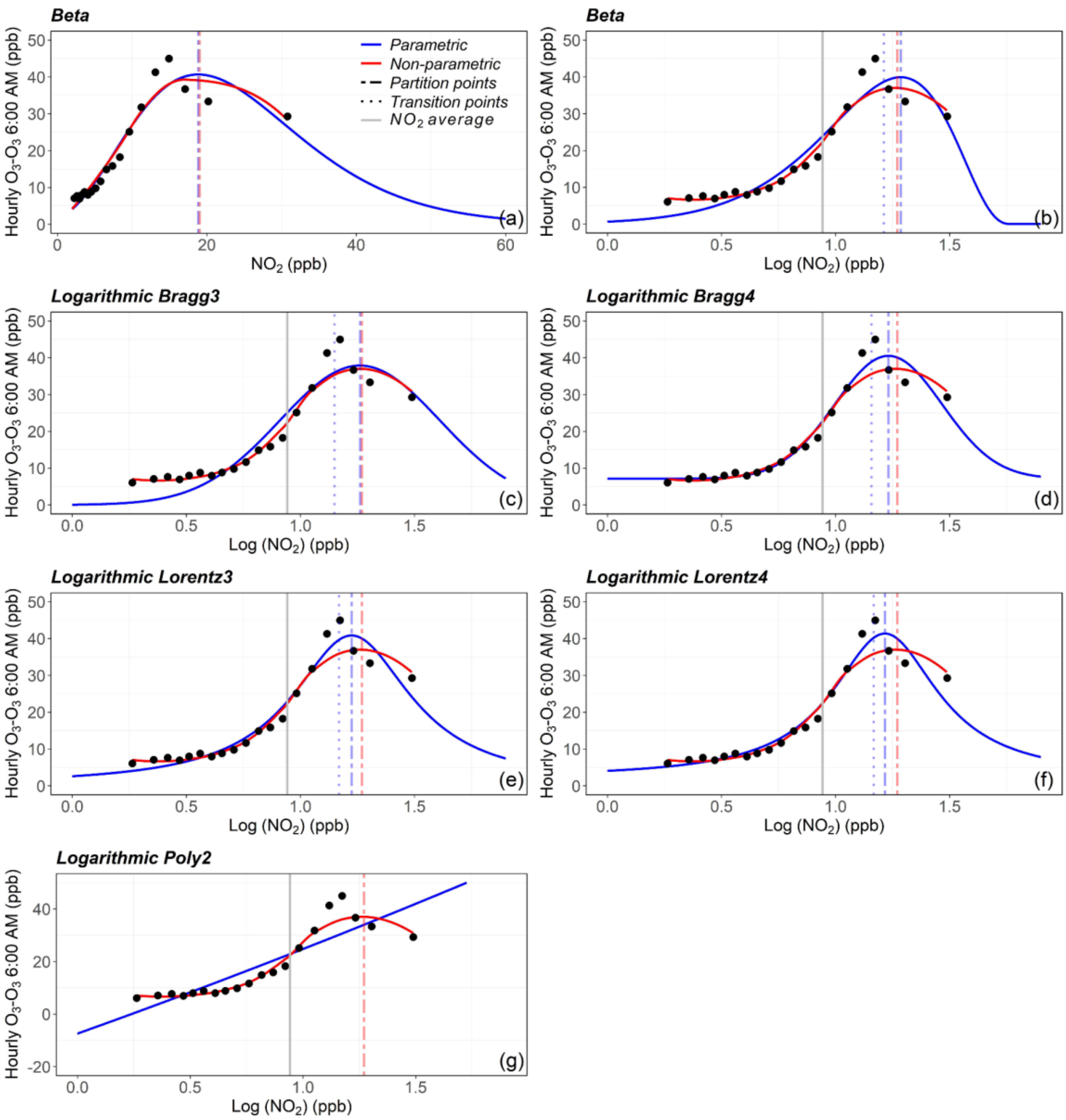

Figure S8 The **DPO$_2$-NO$_2$** curves for the **Macao** (2014-2019) individually fitted by the studied models (Equations 1-7)

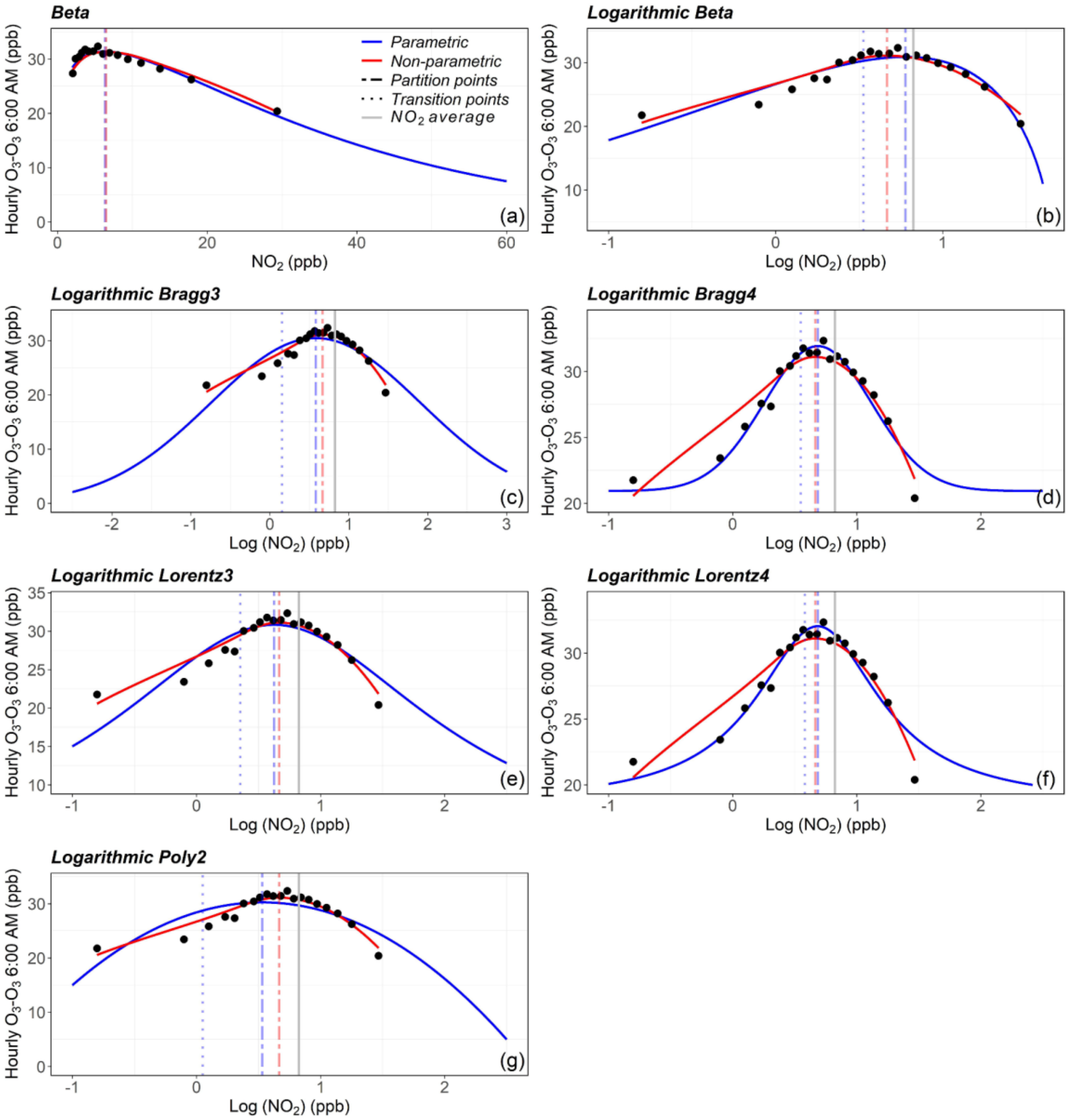

Figure S9 The **DPO3-NO2** curves for the **EU and US** (2014-2019) individually fitted by the studied models (Equations 1-7)

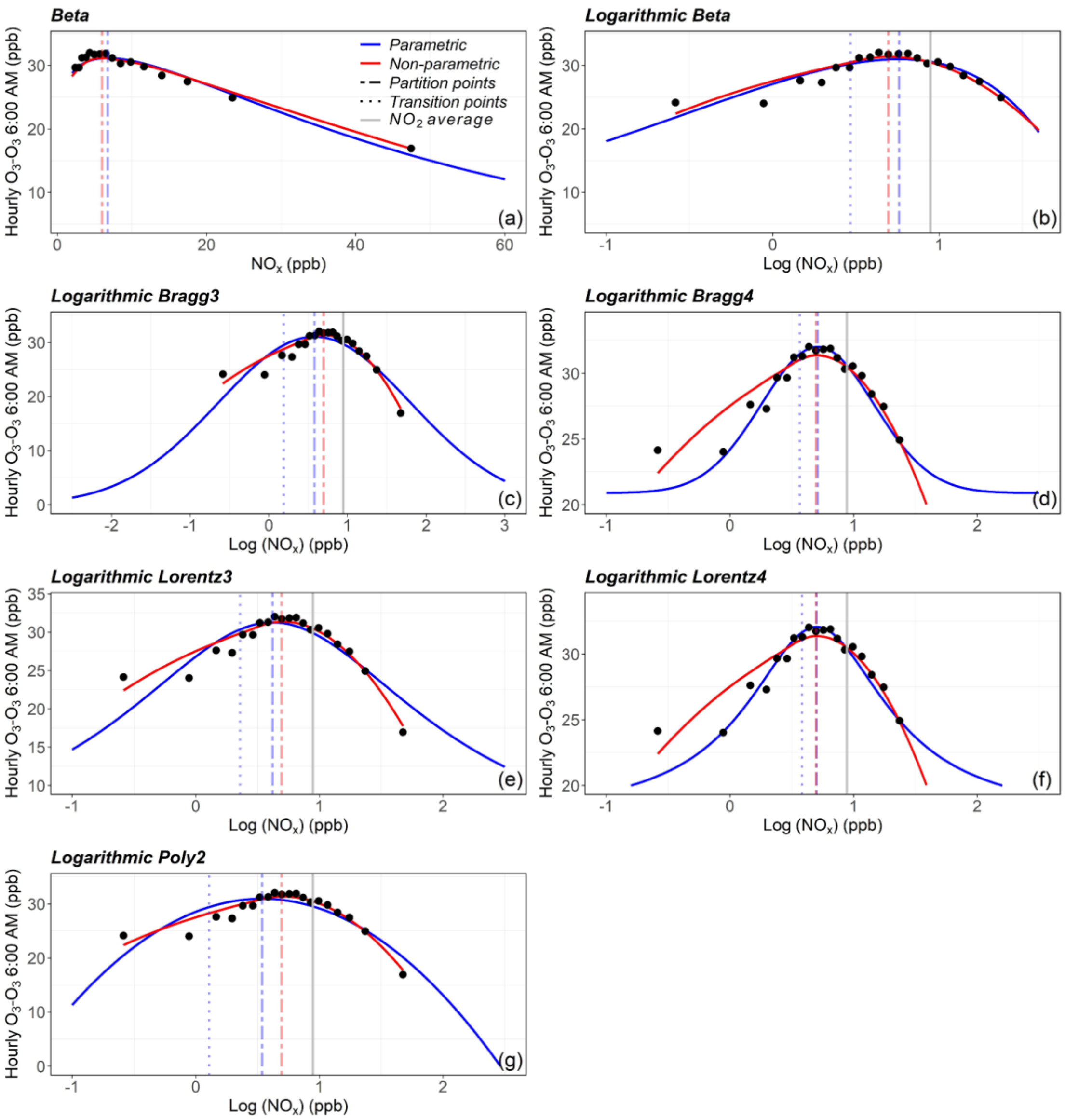

Figure S10 The **DPO_3-NO_x** curves for the **EU and US** (2014-2019) individually fitted by the studied models (Equations 1-7)

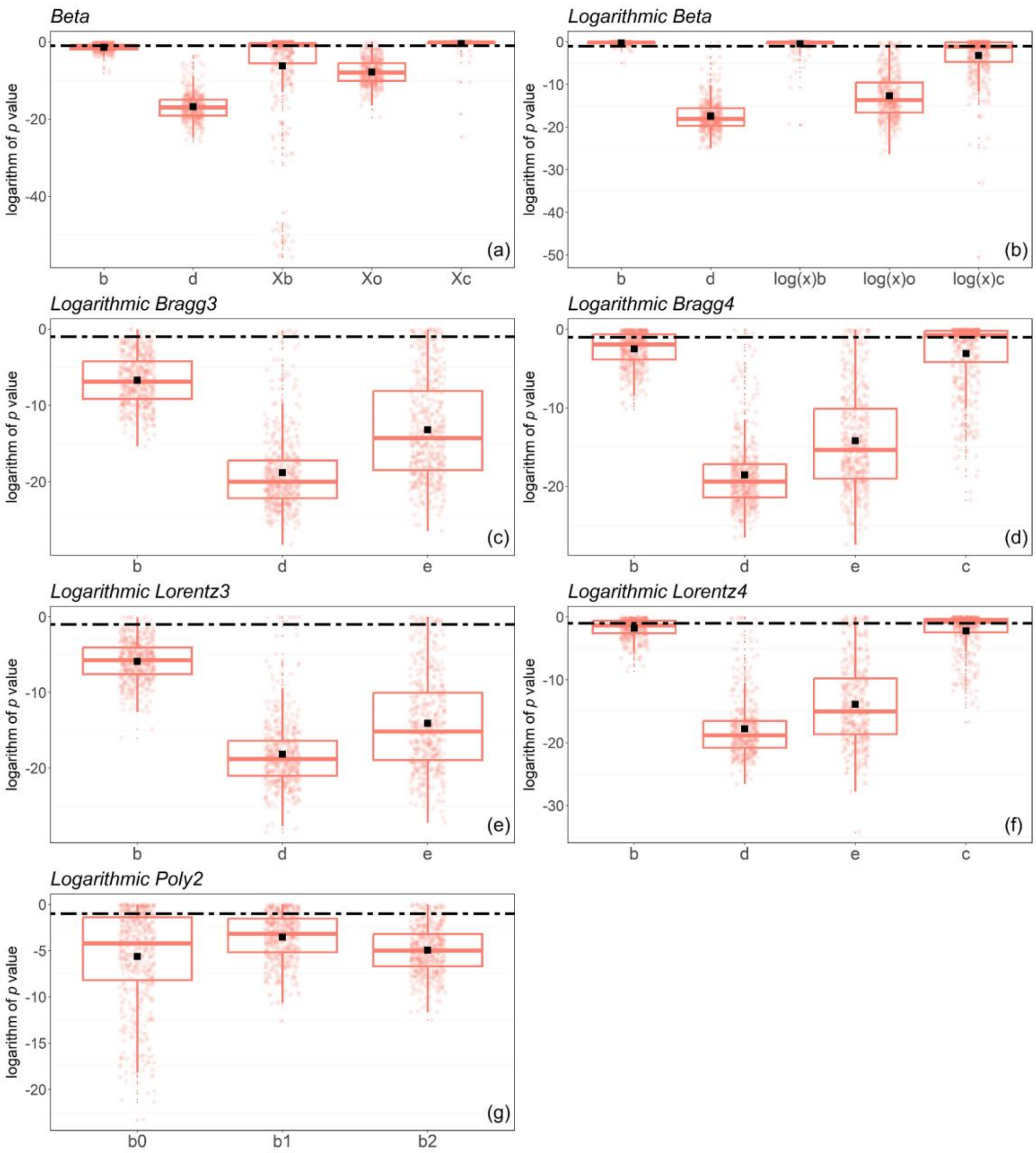

Figure S11 The *p*-values per parameters in the convergent and effective DPO_3-NO_2 fits for **all studied regions**, based on the studied models (Equations 1-7)

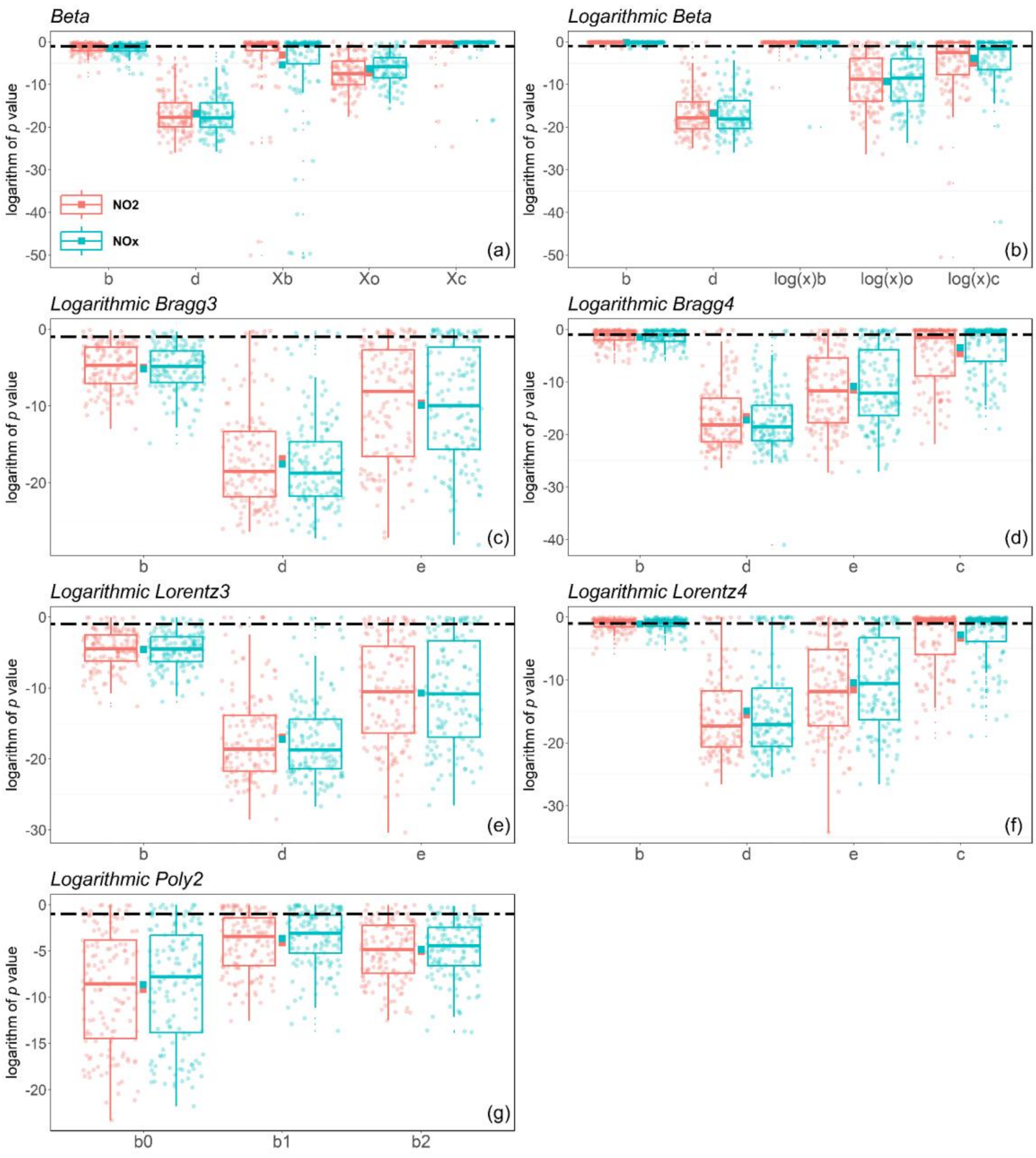

Figure S12 The *p*-values per parameters in the convergent and effective DPO_3-NO_x (or NO_2) fits for **Hong Kong, EU and US**, based on the studied models (Equations 1-7)

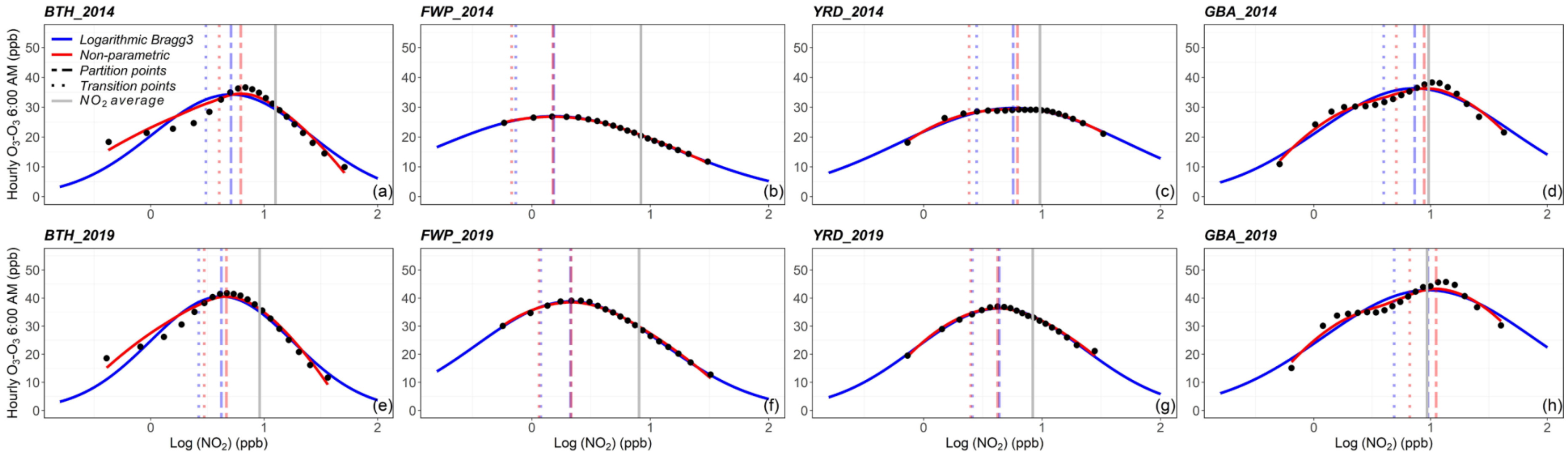

Figure S13 Variations of the DPO3-NO2 curves from 2014 (a-d) to 2019 (e-h) on the regional scale based on the **CAQRA** gridded data. *The gridded data-derived regional DPO_3/NO_2 ratios (BTH: 2.13 in 2014, 3.43 in 2019; FWP: 2.59, 3.81; YRD: 2.84, 3.74; GBA: 3.45, 4.27) were generally higher compared with the observation data, indicating the DPO_3-NO_2 curve is also effective for gridded data. The gridded average NO_2 concentrations were lower than observations (Figure 2, Table S1), reflecting inclusion of lower NO_x-emission areas beyond observation station coverage.* In *GBA (d, h), observation data were prioritized over gridded data for Hong Kong due to poor NO_2 correlation (with a low five-fold cross-validation R^2=0.07) between observation and CAQRA gridded data.*

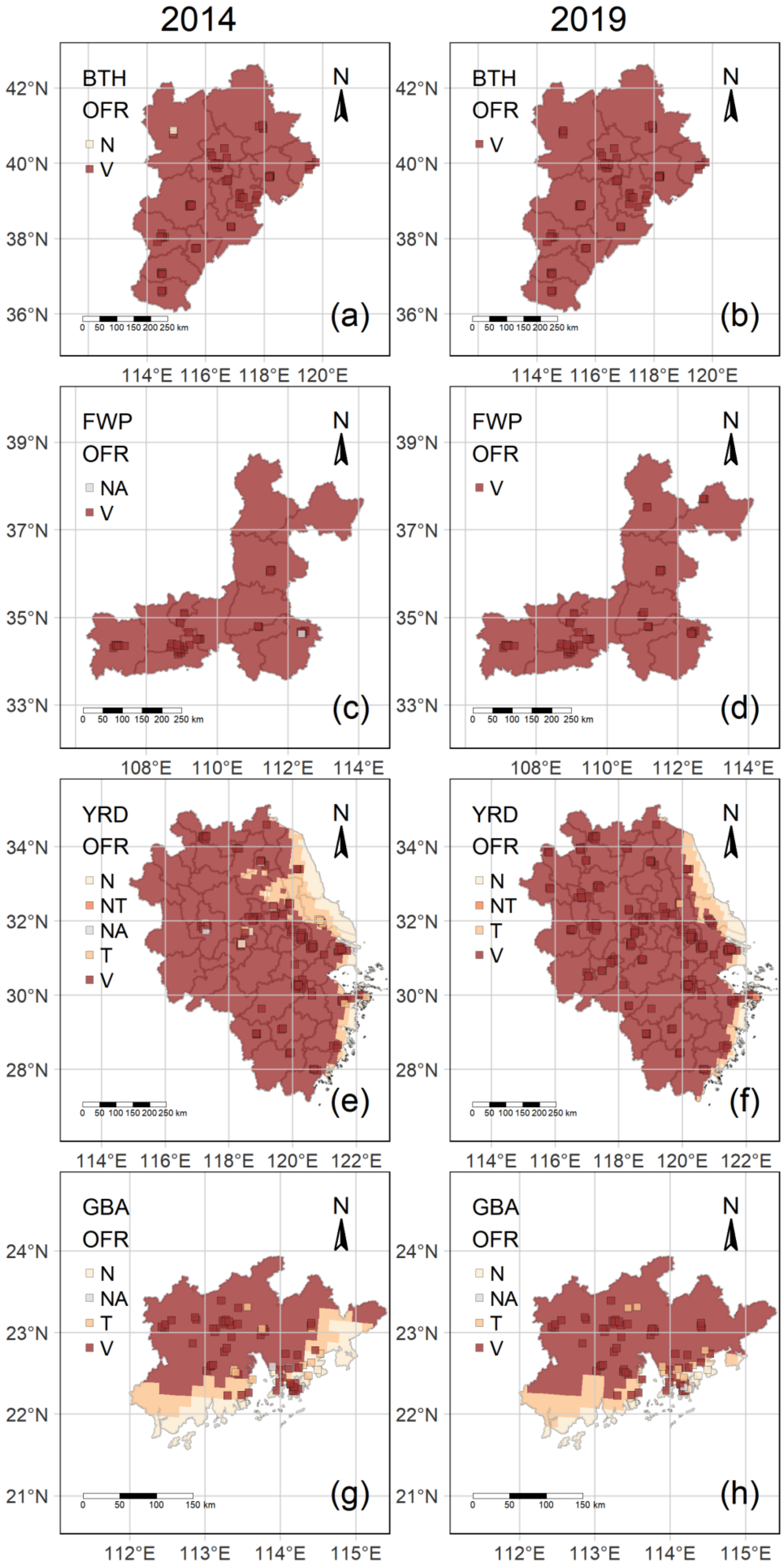
2014
2019
BTH
OFR
N
V
(a)
(b)
FWP
NA
(c)
(d)
YRD
NT
T
(e)
(f)
GBA
(g)
(h)
0 50 100 150 200 250 km
42°N
40°N
38°N
36°N
114°E 116°E 118°E 120°E
39°N
37°N
35°N
33°N
108°E 110°E 112°E 114°E
34°N
32°N
30°N
28°N
114°E 116°E 118°E 120°E 122°E
24°N
23°N
22°N
21°N
112°E 113°E 114°E 115°E
0 50 100 150 km

16

Figure S14 Spatiotemporal variations of the **all-year MDA8-daytime-hour** specific ozone formation regimes (OFRs) from 2014 to 2019 in four city agglomerations of China based on the *logarithmic Bragg 3* model fitting DPO_3-NO_2 curves. *N represented the* NO_x*-limited regime with the stational or gridded average* NO_2 *concentration lower than the transition point; T represented the transition regime with the stational or gridded average* NO_2 *concentration between the transition and partition points; V represented the VOC-limited regime with the stational or gridded average* NO_2 *concentration higher than the partition point; NT denoted the* NO_x*-limited to transition regime, where the* NO_x*-limited and transition regimes cannot be distinguished, as the logarithmic Bragg 3 model fitting curve was irregular (as in Graphical Abstract) but its corresponding linear fit achieved statistical significance (*$p \leq 0.1$*), with the* DPO_3 *monotonically increasing with* NO_2*; NA denoted a non-effective diagnostic result, as the logarithmic Bragg 3 model fitting curve is irregular meanwhile the linear fit is neither statistically significant (*$p > 0.1$*), or there is no valid (stational or gridded) recording following the meteorological screening.*

81 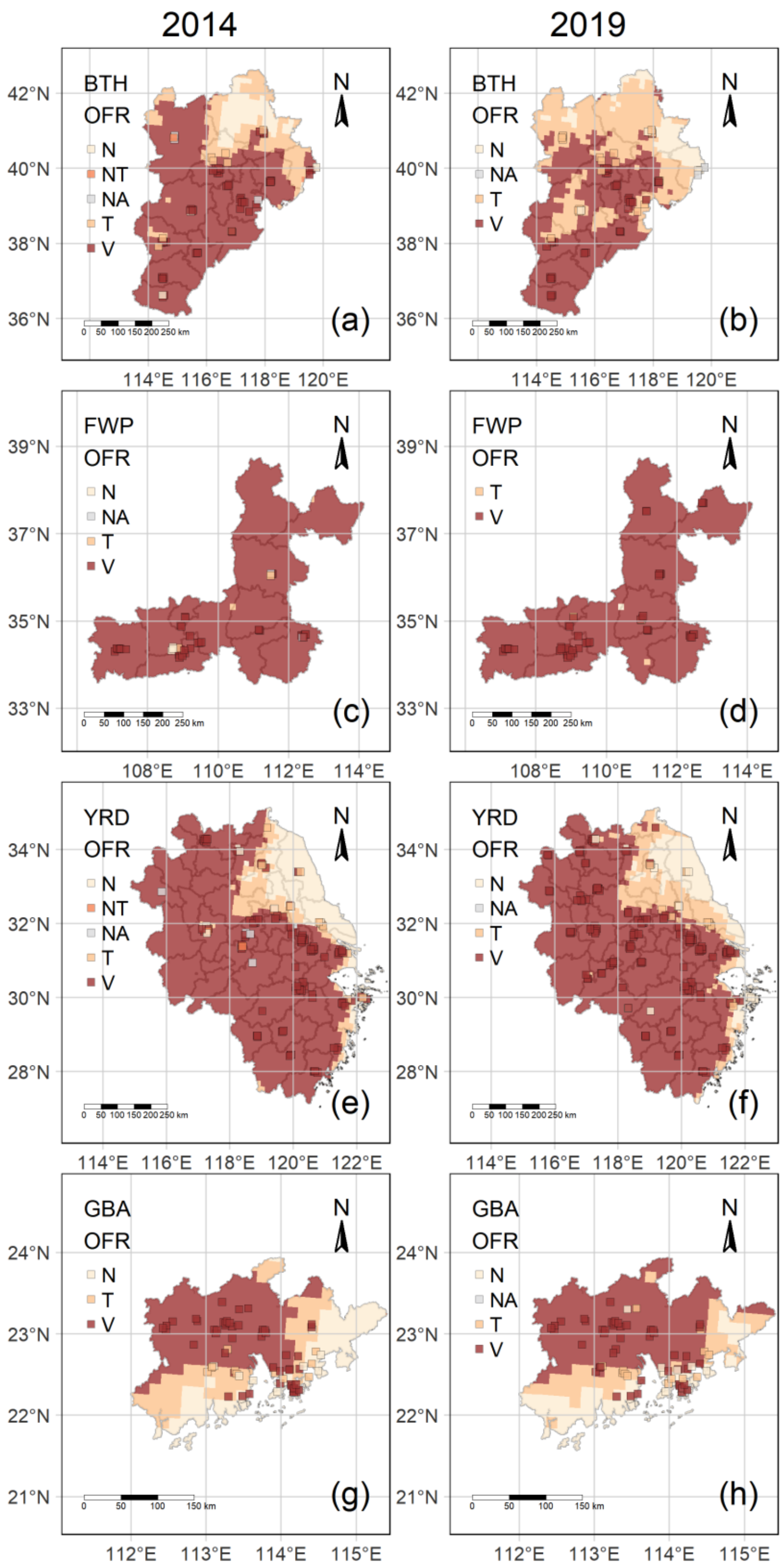

82 Figure S15 The same as Figure S12, but for the **ozone-season midday hours** (April-
83 September, 13:00-14:00 LT)

Table S1 The fitting parameters, average levels (ppb) of NO_2 and DPO_3, partition points (ppb), transition points (ppb), as well as the proportions (%) respectively under the VOC-limited, transition and NO_x-limited regimes specific to **Figure 3**

		BTH		FWP		YRD		GBA		EU		US		EU_US	
		2014	2019	2014	2019	2014	2019	2014	2019	2014	2019	2014	2019	2014	2019
Parameter *b*		1.18	2.42	0.87	1.87	1.00	1.16	0.92	1.33	0.57	0.42	0.31	0.26	0.30	0.32
Parameter *d*		45.07	53.25	34.72	54.78	38.90	45.48	39.59	47.22	10.47	9.97	31.45	30.89	30.54	30.32
Parameter *e*		0.74	0.82	0.56	0.70	0.91	0.77	0.85	1.02	0.17	0.29	0.57	0.66	0.53	0.62
NO_2		18.68	15.51	15.68	15.52	15.55	14.04	18.73	17.66	8.79	7.91	7.24	5.86	7.30	5.95
DPO_3		33.16	38.61	25.54	38.09	33.95	38.11	33.16	41.22	7.71	8.29	29.15	29.23	28.22	28.40
Partition point	Logarithmic Bragg3	5.45	6.60	3.62	5.06	8.23	5.84	7.03	10.60	1.48	1.97	3.74	4.61	3.42	4.16
	Non-parametric	5.56	6.89	3.25	4.86	10.34	6.23	8.58	10.95	1.78	3.67	4.65	5.15	4.42	4.75
Transition point	Logarithmic Bragg3	3.38	4.73	2.08	3.46	4.89	3.61	4.10	6.75	0.74	0.89	1.48	1.66	1.32	1.67
	Non-parametric	2.69	5.54	NA	2.96	5.74	3.24	4.18	7.28	0.80	2.31	2.35	2.56	2.26	2.42
VOC-limited %	Logarithmic Bragg3	82.29	77.63	92.41	87.72	72.10	84.63	79.74	65.10	76.43	75.88	59.00	42.79	61.42	47.68
	Non-parametric	82.29	77.63	93.65	87.72	61.05	82.07	72.94	62.72	73.98	60.85	50.29	38.30	51.75	42.38
Transition %	Logarithmic Bragg3	7.71	12.08	3.13	6.49	13.27	9.62	11.94	18.82	8.35	8.74	26.38	38.56	24.40	33.51
	Non-parametric	8.71	12.08	6.35	8.50	22.18	12.17	18.75	18.94	9.86	11.54	23.70	29.85	22.95	27.21
NO_x-limited %	Logarithmic Bragg3	10.00	10.29	4.46	5.78	14.63	5.75	8.31	16.07	15.22	15.38	14.62	18.65	14.18	18.81
	Non-parametric	8.99	10.29	0	3.77	16.77	5.75	8.32	18.34	16.16	27.60	26.00	31.84	25.29	30.41

Table S2 The fitting parameters, average levels (ppb) of NO_2 and DPO_3, partition points (ppb), transition points (ppb), as well as the proportions (%) respectively under the VOC-limited, transition and NO_x-limited regimes specific to **Figure S13**

		BTH		FWP		YRD		GBA	
		2014	2019	2014	2019	2014	2019	2014	2019
Parameter *b*		1.03	1.27	0.50	0.81	0.54	0.99	0.73	0.62
Parameter *d*		34.26	40.54	26.96	38.78	29.69	36.29	36.31	46.78
Parameter *e*		0.71	0.62	0.18	0.33	0.76	0.64	0.86	0.98
NO_2		12.58	9.12	8.35	8.04	9.60	8.35	9.63	9.34
DPO_3		26.75	31.27	21.62	30.67	27.30	31.25	30.99	37.19
Partition point	Logarithmic Bragg3	5.11	4.20	1.53	2.13	5.71	4.36	7.30	9.49
	Non-parametric	6.23	4.66	1.50	2.15	6.22	4.23	9.89	11.82
Transition point	Logarithmic Bragg3	3.06	2.65	0.73	1.19	2.81	2.58	3.98	4.89
	Non-parametric	4.02	2.95	0.67	1.15	2.41	2.49	5.46	7.08
VOC-limited %	Logarithmic Bragg3	67.01	61.44	86.93	77.89	61.82	66.16	44.09	34.13
	Non-parametric	60.70	57.72	87.23	77.60	58.46	67.26	37.70	28.61
Transition %	Logarithmic Bragg3	11.76	14.06	9.10	11.76	20.77	16.15	18.72	22.18
	Non-parametric	12.71	14.99	9.50	12.64	27.16	15.87	17.89	17.82
NO_x-limited %	Logarithmic Bragg3	21.23	24.50	3.97	10.35	17.41	17.69	37.19	43.69
	Non-parametric	25.59	27.29	3.27	9.76	14.38	16.87	44.41	53.57